Carbohydrate Polymers 117 (2015) 99–105

Contents lists available at ScienceDirect

Carbohydrate Polymers

journal homepage: www.elsevier.com/locate/carbpol

Preparation and characterization of regenerated cellulose from ionic liquid using different methods

Zhenghui Liu [a], Xiaofu Sun [a], Mingyang Hao [a], Chengyi Huang [a], Zhimin Xue [b], Tiancheng Mu [a,*]

[a] Department of Chemistry, Renmin University of China, Beijing 100872, China
[b] College of Materials Science and Technology, Beijing Forestry University, Beijing 100083, China

ARTICLE INFO

Article history:
Received 27 August 2014
Accepted 21 September 2014
Available online 30 September 2014

Keywords:
Cellulose
Ionic liquid
Compressed carbon dioxide
Anti-solvent
Biomass treatment

ABSTRACT

In this study, regenerated cellulose was prepared from ionic liquid 1-butyl-3-methylimidazolium acetate ([Bmim]Ac) solution using anti-solvent compressed CO_2 of different pressures. And other anti-solvents like water, ethanol and acetonitrile were also employed to regenerate cellulose to provide comparisons. The two-dimensional nuclear magnetic resonance (2D NMR), namely heteronuclear single quantum coherence (HSQC) and heteronuclear multiple bond coherence (HMBC), and attenuated total reflectance Fourier transform infrared spectroscopy (ATR–FTIR) indicated that carboxylate zwitterions [$Bmim^+$-COO^-] formed through the chemical reactions between CO_2 and [Bmim]Ac. Besides, FTIR, wide-angle X-ray diffraction (XRD), thermal gravimetric analysis (TGA), differential scanning calorimetry (DSC), scanning electron microscopy (SEM) and transmission electron microscopy (TEM) were used to provided structure characterization of native and regenerated cellulose using different anti-solvents. The results show that the crystallinity of cellulose decreases during the dissolution and regeneration process. And a crystal transformation of cellulose I to cellulose II was verified. The stability of the regenerated cellulose is lower than that of native cellulose. A higher compressed CO_2 pressure results in a smoother surface, a thicker shape and a more homogeneous texture of regenerated cellulose.

1. Introduction

Biomass is an important and renewable energy material on Earth, among which cellulose is the most widespread natural polymer which exists as a useful industrial raw material because it is cheap, chemically stable, nonpoisonous, environmentally friendly, and modifiable (Miller, 2013; Ragauskas et al., 2006). Preparation of valuable products of different kinds from biomass, especially from cellulose, via technically feasible ways has been explored all along (Hama et al., 2014; Qu et al., 2014; Vo, Widyaya, Jae, Kim, & Lee, 2014). But cellulose has strong inter- and intra-molecular hydrogen bonds, which cause it hard to dissolve in common molecular solvents and thus difficult for the subsequent dispositions because dissolution is prerequisite before translating into other desired products in many cases. So in spite of enormous annual production, the difficulty of dissolving would limit its utilization to quite a narrow scope.

The ability of disrupting the interchain hydrogen bonds of cellulose determines the dissolution efficiency of a solvent. Some solvent systems have already been developed to dissolve cellulose, such as thiourea/H_2O or NaOH/urea system, NaOH/CS_2 system, alkali/H_2O system, LiOH/urea/H_2O system, molten salt hydrate system, like $LiSCN{\cdot}2H_2O$ and $LiClO_4{\cdot}3H_2O$, and some other systems like *N*-methylmorpholine-*N*-oxide (NMMO), dimethyl sulfoxide (DMSO)/tetrabutyl ammonium fluoride (TBAF), LiCl/1,3-dimethyl-2-imidazolidinone (DMI), LiCl/*N*-methyl-2-pyrrolidine (NMP) and LiCl/*N*,*N*-dimethylacetamide (DMAc) (Klemm, Heublein, Fink, & Bohn, 2005; Xu, Wang, & Wang, 2010). But these systems always have difficulty in solvent separation and cause environmental pollution. Besides, ionic liquid (IL) can dissolve cellulose to a satisfying concentration (Pinkert, Marsh, Pang, & Staiger, 2009; Swatloski, Spear, Holbrey, & Rogers, 2002). IL is a kind of organic salts with a melting point at or below room temperature which is being considered to have a wide variety of applications in organic synthesis, synthesis of nanomaterials, catalysis, separation analysis and electronchemistry (Petkovic, Seddon, Rebelo, & Pereira, 2011). ILs are composed of only ions that makes most of them own a series of particular physicochemical properties, such as negligible vapor

* Corresponding author. Tel.: +86 1062514925; fax: +86 1062516444.
E-mail addresses: tcmu@chem.ruc.edu.cn, tcmu@ruc.edu.cn (T. Mu).

http://dx.doi.org/10.1016/j.carbpol.2014.09.053
0144-8617/

pressure, outstanding solvation ability, wide temperature for liquid, high thermal stability, designability and wide electrochemical window. Famous for "task-specific" and "tailor-making", ILs are viewed as green solvents and environmentally friendly alternatives for conventional volatile organic solvents by virtue of tailored physical and chemical prosperities by different matches of cations and anions and modifying the functional groups on cations or anions. IL was first used to dissolved cellulose by Swatloski et al. (2002) and after that several ILs with higher dissolving capacity were found (Andanson et al., 2014; Zhang, Wu, Zhang, & He, 2005; Zhao et al., 2008) among which 1-butyl-3-methylimidazolium acetate ([Bmim]Ac) was reported to possess excellent ability to dissolve cellulose (Xu et al., 2010).

It is fairly important that biomass products of various types are separated efficiently but cellulose/IL solution possesses the disadvantage of difficulty in separating and purifying. At present, anti-solvent method performs remarkably in cellulose separation from ILs. For example, ethanol or water, as an anti-solvent, is loaded into the cellulose/IL solution (Xu et al., 2010). Since ethanol and water are miscible with IL but not with cellulose, the solubility of cellulose in IL is significantly lessened and thus we acquire regenerated cellulose. By using conventional anti-solvents, after the cellulose precipitates, molecular solvent and IL are mixed together as a phase thus leaving a troublesome problem of how to separate them due to the strong interactions between IL and anti-solvents. So it is requisite to develop an energy saving, environmentally benign and effective method to regenerate cellulose from IL.

Compressed CO_2, as a cheap, safe, environmentally benign, non flammable medium, has continuously adjusted physical properties from gas-like to liquid-like by changing temperature and pressure, which can be easily recycled after use (Eckert, Knutson, & Debenedetti, 1996; Zhang & Han, 2012). Considerable amount of CO_2 can be absorbed into ILs but cellulose is not soluble in compressed CO_2, which acts as a gas anti-solvent here (Blanchard, Hancu, Beckman, & Brennecke, 1999). Besides, formation of carboxylate zwitterion from [Bmim]Ac and CO_2 contributes to the coagulation of cellulose from [Bmim]Ac (Gurau et al., 2011). Therefore, dissolved cellulose will precipitate from ILs by using compressed CO_2 and a noteworthy benefit is that CO_2 can be easily separated from ILs by depressurization without new problems in separation process, which solves the big problem of the separation of IL and anti-solvent and the issue of recycling.

In our current work, we studied the regeneration of cellulose from [Bmim]Ac using compressed CO_2 as a gas anti-solvent. Because of its outstanding dissolving ability, [Bmim]Ac was used as the solvent of cellulose. Compressed CO_2 of different pressure was loaded into the cellulose solution to receive regenerated cellulose. Besides, water, ethanol and acetonitrile were also used to precipitate cellulose to provide comparisons. Rogers et al. have proposed the method of using compressed CO_2 to regenerate chitin from 1-ethyl-3-methylimidazolium acetate (EmimAc) (Barber et al., 2013), and our previous work gave a further exploration of the systems (Sun, Chi, & Mu, 2014a; Sun, Xue, & Mu, 2014b). And in this work, we probed into the regeneration mechanism and structure characterization of regenerated cellulose using different anti-solvents, compressed CO_2 of different pressure included. Yields of regenerated cellulose were measured. Attenuated total reflectance Fourier transform infrared spectroscopy (ATR–FTIR) and two dimensional nuclear magnetic resonance (2D NMR), namely heteronuclear single quantum coherence (HSQC) and heteronuclear multiple bond coherence (HMBC) were employed to confirm the regeneration mechanism. Beside, Fourier transform infrared spectroscopy (FTIR) and wide-angle X-ray diffraction (XRD) provided structure characterization, and thermal gravimetric analysis (TGA) and differential scanning calorimetry (DSC) were used to give thermal analysis. Finally, scanning electron microscopy (SEM) and transmission electron microscopy (TEM) were applied to morphology observation.

2. Materials and methods

2.1. Materials

The linter cellulose was purchased from Hubei Golden Ring Co., Ltd. (Xiangyang, Hubei Province, China). The cellulose samples were teared into small pieces and dried in a vacuum oven at 80 °C for around 10 h before use. CO_2 (99.999%) was obtained from Beijing Beiwen Gas Chemical Industry Co., Ltd. [Bmim]Ac (99.9 wt%) was received from Lanzhou Greenchem. ILs, LICP, CAS, China (Lanzhou, China). After drying it at 40 °C in a vacuum oven for 48 h, the water content of IL was less than 1000 ppm determined by Karl–Fischer titration. Deionized water was employed throughout the experiments.

2.2. Dissolution of linter cellulose in [Bmim]Ac

Cellulose fragments were added into [Bmim]Ac with portions of 0.2 wt% of ionic liquid every time under continuous stirring at about 100 °C until the concentration of cellulose achieved 10.0 wt% of the IL. Finally, a homogeneous and plained solution was obtained.

2.3. Regeneration of cellulose from [Bmim]Ac using compressed carbon dioxide and other anti-solvents

The cellulose samples dissolved in [Bmim]Ac were put in high-pressure cells with a volume of about 8 ml, respectively, at 25 °C in a water bath with a constant temperature controller (±0.1 °C). Then CO_2 was loaded into the cells after the air in the cells were removed until presupposed pressure was achieved. After 3 h CO_2 was released and aerogels were obtained. Ethanol was used to wash away the IL, and the regenerated cellulose retained, from which we can calculate the yields. In addition, we put the cellulose solutions into water, ethanol and acetonitrile and obtained gels directly and immediately. After further washing with ethanol to remove IL, we got regenerated cellulose.

2.4. Characterization of the regenerated and native cellulose

2.4.1. Yields

Yields were calculated using an electronic analytical balance (Mettler Toledo ML204/actual scale interval = 0.1 mg). Masses of each cellulose sample before dissolution and after regeneration were weighed, respectively.

2.4.2. ATR–FTIR and 2D NMR spectroscopy measurement

Pure and dried ionic liquid [Bmim]Ac of 5 ml was put into the high-pressure cell at 25 °C in a water bath with a constant temperature controller (±0.1 °C). Then CO_2 was loaded into the cells after the air in the cells were removed until presupposed pressure 6.6 MPa was achieved. After keeping for 3 h, redundant CO_2 was released and the pressure reached the normal pressure (0.1 MPa). ATR–FTIR spectroscopy was implemented to investigate structure changes in the liquid phase and our ATR–FTIR measurements were performed on a Prestige-21 FTIR spectrometer (Shimadzu, Japan, DTGS detector) using a single reflection ATR cell (a ZnSe ATR-8200H cell, 584 mm^2 surfaces, 45° incident angles) over the range of 2000–1100 cm^{-1} with a resolution of 4 cm^{-1} and 40 total scans. Besides, 2D NMR (HSQC and HMBC) spectra were acquired with a Bruker Advance 600 MHz spectrometer using a co-axial capillary containing D_2O as a lock solution.

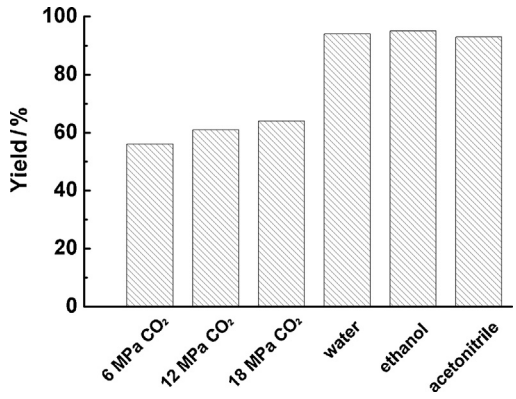

Fig. 1. The yields of regenerated cellulose using different methods.

2.4.3. Structure identification of native and regenerated cellulose

In order to identify the changes of chemical properties and crystal structures during dissolution and subsequent regeneration, FTIR and XRD measurement were performed. FTIR measurement was carried on using Prestige-21 FTIR spectrometer (Shimadzu, Japan) with the KBr disk method (sample/KBr ratio = 1/100). The FTIR spectra were recorded over the range of 4000–400 cm^{-1} with a resolution of 4 cm^{-1} and 40 total scans. XRD patterns of native and regenerated samples were collected by an X-ray diffractometer (Rigaku D/max-2500) using Cu $K\alpha$ as X-ray radiation (λ = 1.5418 Å) under 40 kV and 200 mA. Our scanning range was 2θ = 5–80 degrees with a step of 2θ = 0.02 degree and 0.5 s per step.

2.4.4. Thermal analysis

Thermal analysis was conducted using TGA and DSC to get decomposition temperature (T_d) and glass transition temperature (T_g) of each sample. TGA was performed on Thermogravimetric Analyzer (TA Instrument company, USA) in nitrogen atmosphere (ramp 10 °C/min from room temperature to 800 °C, N_2 flow 40 ml/min and platinum pans). DSC was performed on a DSC Q2000 (TA Instruments, New Castle, DE), equipped with a refrigerated cooling system (RCS 90). Samples were heated at 10 °C/min from room temperature to 200 °C (for native cellulose to 300 °C) in closed alumina crucibles to determine T_gs after removing thermal history.

2.4.5. Morphology observation

The SEM images were collected on a field emission scanning electron microscope JEOL JSM-7401F. The TEM images were performed a transmission electron microscope JEM 1011 to observe the microstructure of the regenerated and native cellulose.

3. Results and discussion

3.1. Cellulose regeneration using compressed CO_2

After adding anti-solvents, dissolved cellulose will be precipitated. The regenerated cellulose share the similar appearances (Fig. S1). And their yields were measured and summarized in Fig. 1. The compressed CO_2 anti-solvents give relatively lower yields of about 60%. Additionally, a higher pressure of compressed CO_2 is associated with a slightly higher yield of regenerated cellulose. In comparison, the conventional anti-solvents such as water, ethanol and acetonitrile show high yields above 90%.

3.2. The mechanisms of regeneration of cellulose

The possible mechanisms of regeneration of cellulose are discussed in this part. 2D NMR (HSQC and HMBC) and ATR–FTIR were employed to confirm the interactions in the system. It is important to judge whether there exist chemical reactions between [Bmim]Ac and CO_2, since a good deal of CO_2 can be absorbed into [Bmim]Ac. Carboxylate zwitterions imidazolium-2-carboxylate ([$Bmim^+$-COO^-]) can be formed through the chemical reactions between CO_2 and [Bmim]Ac, which cause the hydrogen bonds between cellulose and [Bmim]Ac disrupted and thus leading to the regeneration of cellulose from cellulose/[Bmim]Ac solution.

So as to explore the mechanism of regeneration of cellulose by using compressed CO_2, we compared 2D NMR (HSQC and HMBC) spectra of pure [Bmim]Ac and [Bmim]Ac charged with compressed CO_2 of 6.6 MPa for 3 h. As shown in Fig. 2, new ^1H resonances at 3.90 ppm and 4.42 ppm can be attributed to the formation of carboxylate zwitterions imidazolium-2-carboxylate ([$Bmim^+$-COO^-]).(Besnard et al., 2012) We can conclude that the acidic proton at C(2) position on the imidazolium ring may generate a chemical exchange to the acetate anion, and this equilibrium can be disturbed by the carboxylation reaction after charging CO_2, leading to the formation of a CO_2–carbene intermediate and the new species of [$Bmim^+$-COO^-]. Since the formation of carboxylate zwitterion may remove two acetate anions to form a dimer, IL cannot be qualified for the corresponding hydrogen bond acceptor efficiently, leading to the regeneration of cellulose from IL.

Additionally, [Bmim]Ac shows new ^{13}C resonance after charging CO_2, which is 152.85 ppm. The origin of the new resonance is clearly connected with the adding of CO_2. As the isolated CO_2 has a single resonance at 125.4 ppm, (O'Leary, Jaworski, & Hartman, 1979) this new resonance cannot correspond to the CO_2 molecule that dissolved into the acetate-based ILs directly. It seems that it can be attributed to the reactions between CO_2 and the acetate-based ILs. So we can propose a reaction scheme occurring between CO_2 and [Bmim]Ac.

In the meantime, ATR–FTIR measurements were conducted in order to further confirm the species changes of the system. Fig. S2 exhibits the ATR–FTIR spectra of pure [Bmim]Ac and [Bmim]Ac loaded with CO_2 of 6.6 MPa for 3 h to provide comparison so as to verify the the formation of carboxylate zwitterions imidazolium-2-carboxylate ([$Bmim^+$-COO^-]). An extra peak appears at about 1650 cm^{-1} in the curve a (corresponding to [Bmim]Ac after charging CO_2) compared with curve b (corresponding to pure [Bmim]Ac). Since isolated CO_2 absorbs near 2360 cm^{-1}, and the typical COO^- and COOH absorb in the range of 1350–1450 cm^{-1} and 1680–1750 cm^{-1}, respectively, the new peak cannot root in isolated CO_2 molecule dissolved in [Bmim]Ac, typical COO^- or COOH formed after charging CO_2. So it is attributed to the reaction between CO_2 and [Bmim]Ac and the formation of carboxylate zwitterions imidazolium-2-carboxylate ([$Bmim^+$-COO^-]).

As exhibited in Fig. 3, the carboxylation reaction here is a process of two stages. As the first step, proton at C(2) of the [Bmim] cation exchanges to the acetate anion from the imidazolium ring forming an acetic acid molecule while the deprotonated [Bmim] cation turns into imidazole-2-ylidene carbene. In the second step, carbene intermediate attacks CO_2 leading to the formation of carboxylate zwitterions imidazolium-2-carboxylate ([$Bmim^+$-COO^-]). The proton released from the imidazolium ring participates in the formation of a dimer from two acetate anions.

Besides, as revealed in our previous study, (Sun et al., 2014a) loading of compressed CO_2 can cause volume expansion of cellulose/[Bmim]Ac solution which will impel the distance between cellulose and [Bmim]Ac to move longer. Cellulose molecules will come to a more favorable region due to the attractive intermolecular force of the compressed CO_2. CO_2 molecules may encompass cellulose molecules in abundance and thus facilitate the regeneration of cellulose from cellulose/[Bmim]Ac solution. When the cellulose/[Bmim]Ac solution is changed with compressed CO_2, long chain cellulose with larger molecular weight is more easily to be surrounded by CO_2 molecules leading to a poorer interaction with

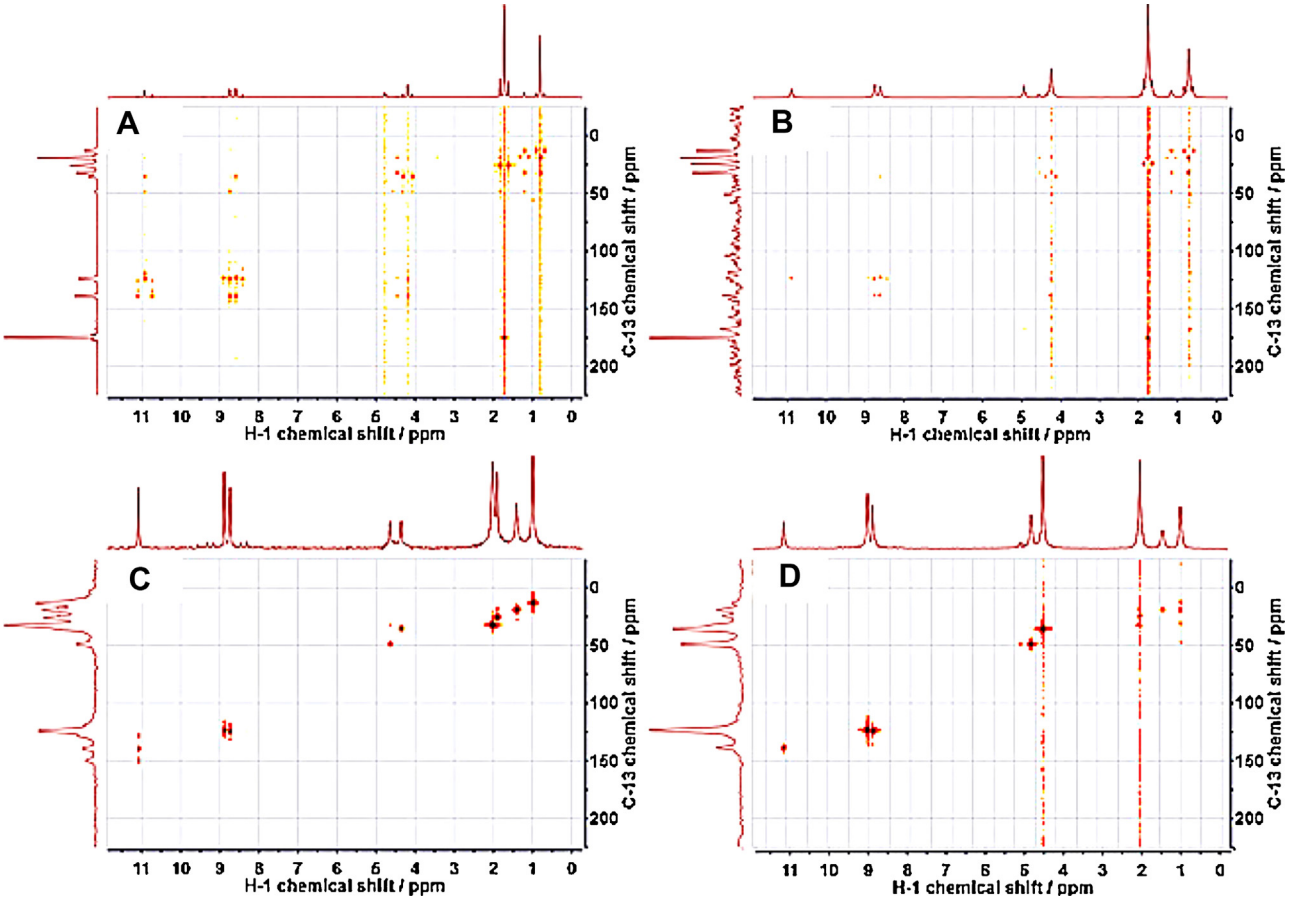

Fig. 2. 2D NMR spectra ((A) HMBC for pure IL (B) HMBC for IL with CO_2 (C) HSQC for pure IL (D) HSQC for IL with CO_2) Figure provides NMR information of new species in the systems.

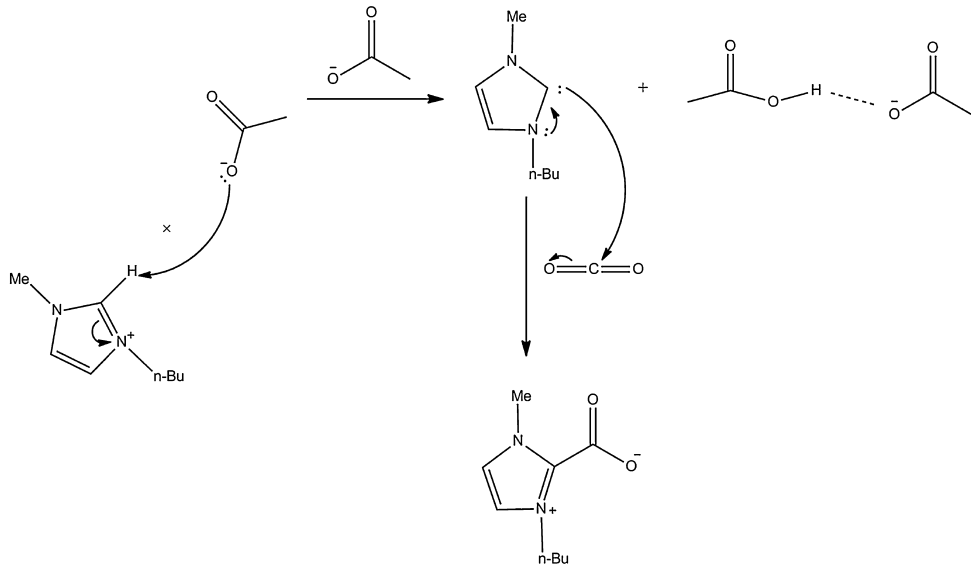

Fig. 3. Mechanism of formation of carboxylate zwitterions imidazolium-2-carboxylate ([$Bmim^+$-COO^-]). Figure explains the process of regeneration and points out the chemical reactions occurring in the systems.

[Bmim]Ac, thus resulting in an easier regeneration. Considering that the compressed CO_2 anti-solvent process can be tuned by changing pressure, temperature and reaction time, the degree of polymerization values of regenerated cellulose can be controlled efficiently and the so-called "staged bio-refining of cellulose" might be realized.

3.3. Structural identifications of the regenerated and the native cellulose

According to previous literatures, (Xu et al., 2010; Zhao, Greiner, & Leitner, 2012) acetate-based ILs, such as [Bmim]Ac, can dissolve cellulose to a satisfying concentration easily and directly. And then

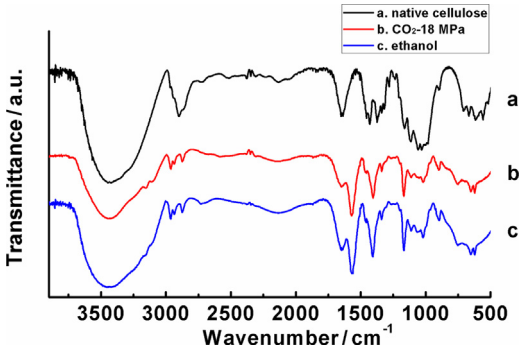

Fig. 4. FTIR spectra of native and regenerated cellulose. Figure identifies the structure of native and regenerated cellulose.

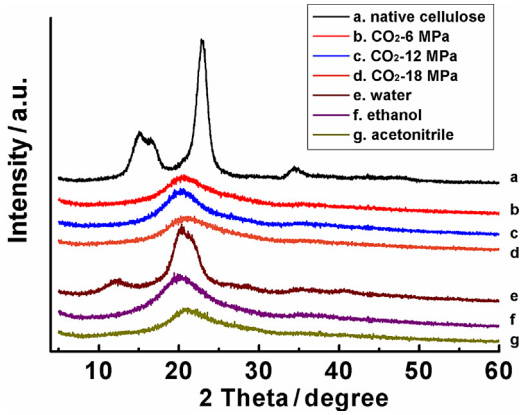

Fig. 5. XRD patterns of native and regenerated cellulose. Figure offers information about crystal structure.

various anti-solvents, compressed CO_2 included, were employed to regenerate cellulose from [Bmim]Ac solution. In order to visualize the changes of molecular interactions and structural modification occurring during dissolution and subsequent regeneration, we conducted FTIR and XRD measurements on the native and the regenerated cellulose using different anti-solvent. And Fig. 4 shows the absorption spectra of them in the range of 4000–500 cm^{-1}. 4000–2995 cm^{-1} region stands for the stretching vibrations of the OH groups presented as broad bands and —CH_2— was observed at 2900 cm^{-1}. The C—O—C bending and the C—H stretching vibration were from 1170 to 1082 cm^{-1} and from 1060 to 1050 cm^{-1}, respectively. And the three IR spectra of native cellulose (Fig. 4a), cellulose regenerated from compressed CO_2 of 18 MPa (Fig. 4b) and ethanol (Fig. 4c) all match the major functional groups of cellulose (Johar, Ahmad, & Dufresne, 2012; Oh, Yoo, Shin, & Seo, 2005). Therefore it can be concluded that the chemical structure of cellulose remained unchanged after dissolution and regeneration, which indicates that [Bmim]Ac is a nonderivative solvent in the meantime.

Almost no differences can be found between the spectra of regenerated cellulose using compressed CO_2 of 18 MPa (Fig. 4b) and ethanol (Fig. 4c). However, the native cellulose has a spectrum (Fig. 4a) with a few differences from those of regenerated cellulose, which reflects the variation of cellulose crystallization. For example, a small sharp band at 895 cm^{-1}, representing the C—O—C asymmetric stretching, is enhanced in the spectra of regenerated cellulose using compressed CO_2 of 18 MPa and ethanol compared to the spectrum of native cellulose, while the peak at 1430 cm^{-1} representing the CH_2 scissoring motion, is weakened. It is worth noting that the peak at 895 cm^{-1} stands for the amorphous absorption band and is usually more pronounced in amorphous and cellulose II, while the peak at 1430 cm^{-1} stands for the crystalline absorption band and is usually more pronounced in cellulose I (Adsul, Soni, Bhargava, & Bansal, 2012; Kuo & Lee, 2009). Therefore we come to a conclusion of a crystal transformation of cellulose I to cellulose II occurring in the process of regeneration.

The XRD profiles of regenerated cellulose from cellulose/[Bmim]Ac (10 wt%) solutions along with native cellulose are shown in Fig. 5. It is easily found that the native cellulose has a special diffraction pattern different from those of regenerated cellulose. There exist four diffraction peaks, namely $2\theta = 14.9$, 16.7, 22.8, 34.5 degrees, in the XRD pattern of native cellulose corresponding to the (-1 1 0), (1 1 0), (2 0 0), and (0 0 4) crystallographic planes, which indicates that the native cellulose crystal belongs to cellulose I (Sebe, Ham-Pichavant, Ibarboure, Koffi, & Tingaut, 2012). However, the regenerated cellulose merely present a wide and plant peak of around $2\theta = 20.4$ degrees, corresponding to (1 1 0) crystallographic planes (Sebe et al., 2012), which indicates that the native cellulose has a higher crystallization degree than the regenerated ones and verifies a crystal transformation from cellulose I to cellulose II after regeneration which is in consistence of our FTIR results. These results reveal that the crystal structure of native cellulose is partially remained in the regenerated cellulose, which is caused by the cleavage of the inter- and intra-molecular hydrogen bonds in the native cellulose during the process of dissolution and the partial reconstitution of hydrogen bond networks of the regenerated cellulose during the course of precipitation. As revealed in other literatures, native cellulose (cellulose I) can change into cellulose II by a recrystallation process. That is to say, the regeneration process converts the crystalline structure from cellulose I to cellulose II (Pang, Liu, Zhang, Wu, & Sun, 2013). There are hydrogen bonds among chains in cellulose I which exist merely in the same sheet (Nishiyama, Sugiyama, Chanzy, & Langan, 2003). However, cellulose II possesses hydrogen bonds among sheets, manifesting a three-dimensional (3D) network (Langan, Nishiyama, & Chanzy, 1999), which makes cellulose II, compared with other cellulose structure, the most stable crystal structure(Lee, Doherty, Linhardt, & Dordick, 2009).

Among the regenerated samples, cellulose regenerated using water as an anti-solvent looks different from those using other anti-solvents in the XRD patterns. That is to say, XRD profiles of regenerated cellulose using compressed CO_2 of various pressures, ethanol and acetonitrile as anti-solvents strongly resemble each other. But XRD profile of regenerated cellulose using water as an anti-solvent, in contrast, has a significantly higher peak at about $2\theta = 20.4$ degrees and an extra peak at $2\theta = 12.2$ degrees corresponding to $(\bar{1}10)$ crystallographic planes of cellulose II. Thus we obtain a conclusion that cellulose regenerated by water owns a relatively higher crystallinity than those by other anti-solvents, which can be explained by the relatively more contribution of water in the formation of hydrogen bonds and the reconstitution of crystal structure during the process of regeneration compared with other anti-solvents used in this experiment.

3.4. Thermal analysis

TGA and DSC were employed to conduct thermal analysis of our samples and the thermal analysis results were summarized in Table 1. TGA curves of the regenerated and the native cellulose samples are shown in Fig. S3. Each cellulose sample experienced a small weight loss before 100 °C because cellulose absorbs water when exposed in the air and it is the stage for evaporation of the absorbed water in cellulose. Then each sample reached its decomposition temperature (T_d) and thus suffered a sharp weight loss due to the pyrolysis of polysaccharide chain. As summarized in Table 1, sample of native cellulose has a T_d of 300.15 °C, while samples of regenerated cellulose own T_ds at around 180–190 °C.

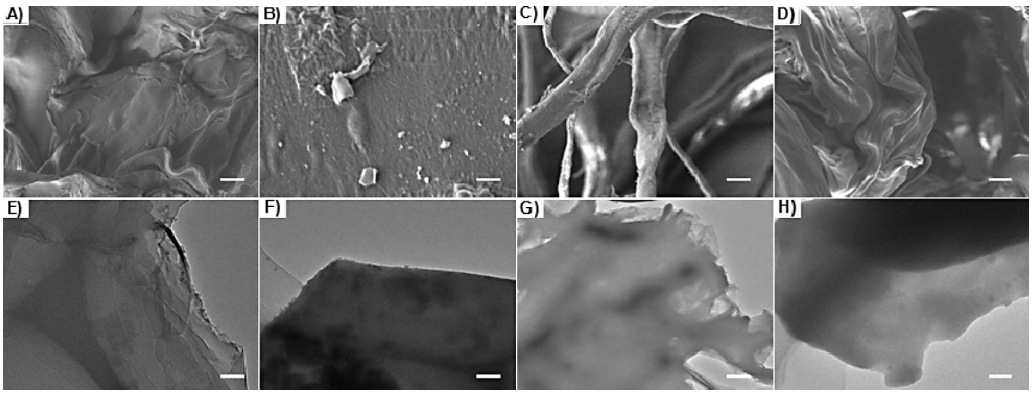

Fig. 6. SEM images ((A) regenerated cellulose using compressed CO_2 of 12 MPa (B) regenerated cellulose using compressed CO_2 of 18 MPa (C). native cellulose (D). regenerated cellulose using ethanol; a scale bar of 2 μm) and TEM images ((E) regenerated cellulose using compressed CO_2 of 12 MPa (F). regenerated cellulose using compressed CO_2 of 18 MPa (G) native cellulose (H) regenerated cellulose using ethanol; a scale bar of 100 nm) Figure gives morphology observation.

Table 1
Thermal analysis of regenerated and native cellulose.

Entry	Anti-solvent	T_d (°C)	T_g (°C)
1	–[a]	300.15	160.99
2	Compressed CO_2-6 MPa	183.76	160.72
3	Compressed CO_2-12 MPa	185.08	160.95
4	Compressed CO_2-18 MPa	184.07	161.32
5	Water	192.34	162.54
6	Ethanol	186.56	160.89
7	Acetonitrile	182.27	160.75

[a] Native cellulose.

This indicates that the processes of dissolution and subsequent regeneration may partially destroyed the hydrogen bond networks and crystal structures of cellulose and are responsible for the decrease of thermal stability of cellulose. The partial reconstitution of cellulose crystal structure in the course of regeneration changed the structure and properties of native cellulose leading to a relatively easier subsequent disposition. Regenerated cellulose using water seems particular because of its higher T_d. Consist with XRD results, water as an anti-solvent can help more in the rebuilding of the hydrogen bond network and crystal structure.

3.5. Morphology observation of the regenerated and the native cellulose

SEM and TEM images of cellulose samples are presented in Fig. 6. Native cellulose has a threadlike appearance (Fig. 6C). And the pressure of compressed CO_2 also makes a difference to the morphology of the regenerated cellulose. Compared to cellulose regenerated using compressed CO_2 of 12 MPa (Fig. 6A), cellulose regenerated using compressed CO_2 of 18 MPa (Fig. 6B) has a smoother surface. And cellulose regenerated using ethanol shows a nubbly surface (Fig. 6D and H). Regenerated cellulose using compressed CO_2 owns a sheet structure, and the sheets seem to grow thicker with the increasing of the pressure of compressed CO_2 used (Fig. 6E and F), which is the result of cellulose accumulation. Compressed CO_2 of higher pressure pushes cellulose out of the cellulose/[Bmim]Ac solution via physical and chemical interactions more thoroughly and thus leaves a thick structure due to the more accumulation of cellulose in the same time. What is more, a thicker sheet structure is associated with a smoother surface with a homogeneous texture. The morphologies of cellulose regenerated using conventional anti-solvents, such as water, ethanol and acetonitrile, resemble each other with a massive and agglomerate texture (see Supplementary data Fig. S4). Regeneration using compressed CO_2 is a gradual process in which cellulose precipitates little by little forming a sheet structure, while regeneration using conventional anti-solvents, such as water, ethanol and acetonitrile is a momentary process in which cellulose precipitates all together forming a bulk structure. That causes the morphology differences between cellulose regenerated using compressed CO_2 and conventional anti-solvents.

4. Conclusions

In summary, an efficient and sustainable method of anti-solvents for regenerate cellulose from ionic liquid was proposed. Compress CO_2 anti-solvents show lower yields. A mechanism for regeneration of cellulose—the formation of carboxylate zwitterions imidazolium-2-carboxylate ([$Bmim^+$-COO^-]) was given. Structure characterization reveals the decrease of the crystallinity of cellulose during the dissolution and regeneration process. And a crystal transformation of cellulose I to cellulose II was verified. The regenerated cellulose owns a lower thermodynamic stability compared to native cellulose. A higher pressure of compressed CO_2 results in a smoother surface, a thicker shape and a more homogeneous texture of regenerated cellulose.

Acknowledgement

Financial support from the National Natural Science Foundation of China (No. 21473252) is greatly appreciated.

Appendix A. Supplementary data

Supplementary data associated with this article can be found, in the online version, at http://dx.doi.org/10.1016/j.carbpol.2014.09.053.

References

Adsul, M., Soni, S. K., Bhargava, S. K., & Bansal, V. (2012). Facile approach for the dispersion of regenerated cellulose in aqueous system in the form of nanoparticles. *Biomacromolecules*, *13*, 2890–2895.

Andanson, J.-M., Bordes, E., Devemy, J., Leroux, F., Padua, A. A. H., & Gomes, M. F. C. (2014). Understanding the role of co-solvents in the dissolution of cellulose in ionic liquids. *Green Chemistry*, *16*, 2528–2538.

Barber, P. S., Griggs, C. S., Gurau, G., Liu, Z., Li, S., Li, Z. X., et al. (2013). Coagulation of chitin and cellulose from 1-ethyl-3-methylimidazolium acetate ionic-liquid solutions using carbon dioxide. *Angewandte Chemie International Edition*, *52*, 12350–12353.

Besnard, M., Cabaco, M. I., Chavez, F. V., Pinaud, N., Sebastiao, P. J., Coutinho, J. A. P., et al. (2012). CO_2 in 1-butyl-3-methylimidazolium acetate. 2. NMR investigation of chemical reactions. *Journal of Physical Chemistry A*, *116*, 4890–4901.

Blanchard, L. A., Hancu, D., Beckman, E. J., & Brennecke, J. F. (1999). Green processing using ionic liquids and CO_2. *Nature*, *399*, 28–29.

Eckert, C. A., Knutson, B. L., & Debenedetti, P. G. (1996). Supercritical fluids as solvents for chemical and materials processing. *Nature*, *383*, 313–318.

Gurau, G., Rodriguez, H., Kelley, S. P., Janiczek, P., Kalb, R. S., & Rogers, R. D. (2011). Demonstration of chemisorption of carbon dioxide in 1,3-dialkylimidazolium acetate ionic liquids. *Angewandte Chemie International Edition*, *50*, 12024–12026.

Hama, S., Nakano, K., Onodera, K., Nakamura, M., Noda, H., & Kondo, A. (2014). Saccharification behavior of cellulose acetate during enzymatic processing for microbial ethanol production. *Bioresource Technology*, *157*, 1–5.

Johar, N., Ahmad, I., & Dufresne, A. (2012). Extraction, preparation and characterization of cellulose fibres and nanocrystals from rice husk. *Industrial Crops and Products*, *37*, 93–99.

Klemm, D., Heublein, B., Fink, H. P., & Bohn, A. (2005). Cellulose: Fascinating biopolymer and sustainable raw material. *Angewandte Chemie International Edition*, *44*, 3358–3393.

Kuo, C.-H., & Lee, C.-K. (2009). Enhancement of enzymatic saccharification of cellulose by cellulose dissolution pretreatments. *Carbohydrate Polymers*, *77*, 41–46.

Langan, P., Nishiyama, Y., & Chanzy, H. (1999). A revised structure and hydrogen-bonding system in cellulose II from a neutron fiber diffraction analysis. *Journal of the American Chemical Society*, *121*, 9940–9946.

Lee, S. H., Doherty, T. V., Linhardt, R. J., & Dordick, J. S. (2009). Ionic liquid-mediated selective extraction of lignin from wood leading to enhanced enzymatic cellulose hydrolysis. *Biotechnology and Bioengineering*, *102*, 1368–1376.

Miller, S. A. (2013). Sustainable polymers: Opportunities for the next decade. *ACS Macro Letters*, *2*, 550–554.

Nishiyama, Y., Sugiyama, J., Chanzy, H., & Langan, P. (2003). Crystal structure and hydrogen bonding system in cellulose 1(alpha), from synchrotron X-ray and neutron fiber diffraction. *Journal of the American Chemical Society*, *125*, 14300–14306.

O'Leary, M. H., Jaworski, R. J., & Hartman, F. C. (1979). ^{13}C nuclear magnetic resonance study of the CO_2 activation of ribulosebisphosphate carboxylase from *Rhodospirillum rubrum*. *Proceedings of the National Academy of Sciences United States of America*, *76*, 673–675.

Oh, S. Y., Yoo, D. I., Shin, Y., & Seo, G. (2005). FTIR analysis of cellulose treated with sodium hydroxide and carbon dioxide. *Carbohydrate Research*, *340*, 417–428.

Pang, J., Liu, X., Zhang, X., Wu, Y., & Sun, R. (2013). Fabrication of cellulose film with enhanced mechanical properties in ionic liquid 1-allyl-3-methylimidaxolium chloride (AmimCl). *Materials*, *6*, 1270–1284.

Petkovic, M., Seddon, K. R., Rebelo, L. P. N., & Pereira, C. S. (2011). Ionic liquids: A pathway to environmental acceptability. *Chemical Society Reviews*, *40*, 1383–1403.

Pinkert, A., Marsh, K. N., Pang, S., & Staiger, M. P. (2009). Ionic liquids and their interaction with cellulose. *Chemical Reviews*, *109*, 6712.

Qu, Y., Wei, Q., Li, H., Oleskowicz-Popiel, P., Huang, C., & Xu, J. (2014). Microwave-assisted conversion of microcrystalline cellulose to 5-hydroxymethylfurfural catalyzed by ionic liquids. *Bioresource Technology*, *162*, 358–364.

Ragauskas, A. J., Williams, C. K., Davison, B. H., Britovsek, G., Cairney, J., Eckert, C. A., et al. (2006). The path forward for biofuels and biomaterials. *Science*, *311*, 484–489.

Sebe, G., Ham-Pichavant, F., Ibarboure, E., Koffi, A. L., & Tingaut, P. (2012). Supramolecular structure characterization of cellulose II nanowhiskers produced by acid hydrolysis of cellulose I substrates. *Biomacromolecules*, *13*, 570–578.

Sun, X., Chi, Y., & Mu, T. (2014). Studies on staged precipitation of cellulose from an ionic liquid by compressed carbon dioxide. *Green Chemistry*, *16*, 2736–2744.

Sun, X., Xue, Z., & Mu, T. (2014). Precipitation of chitosan from ionic liquid solution by the compressed CO_2 anti-solvent method. *Green Chemistry*, *16*, 2102–2106.

Swatloski, R. P., Spear, S. K., Holbrey, J. D., & Rogers, R. D. (2002). Dissolution of cellulose with ionic liquids. *Journal of the American Chemical Society*, *124*, 4974–4975.

Vo, H. T., Widyaya, V. T., Jae, J. H., Kim, H. S., & Lee, H. (2014). Hydrolysis of ionic cellulose to glucose. *Bioresource Technology*, http://dx.doi.org/10.1016/j.biortech.2014.06.025

Xu, A. R., Wang, J. J., & Wang, H. Y. (2010). Effects of anionic structure and lithium salts addition on the dissolution of cellulose in 1-butyl-3-methylimidazolium-based ionic liquid solvent systems. *Green Chemistry*, *12*, 268–275.

Zhang, H., Wu, J., Zhang, J., & He, J. S. (2005). 1-Allyl-3-methylimidazolium chloride room temperature ionic liquid: A new and powerful nonderivatizing solvent for cellulose. *Macromolecules*, *38*, 8272–8277.

Zhang, J., & Han, B. (2012). Supercritical or compressed CO_2 as a stimulus for tuning surfactant aggregations. *Accounts of Chemical Research*, *46*, 425–433.

Zhao, B., Greiner, L., & Leitner, W. (2012). Cellulose solubilitiesin carboxylate-based ionic liquids. *RSC Advances*, *2*, 2476–2479.

Zhao, H., Baker, G. A., Song, Z. Y., Olubajo, O., Crittle, T., & Peters, D. (2008). Designing enzyme-compatible ionic liquids that can dissolve carbohydrates. *Green Chemistry*, *10*, 696–705.